

COVID19-ResCapsNet: A Novel Residual Capsule Network for COVID-19 Detection from Chest X-Ray Scans Images

Dr. Santhosh Kumar S

Associate Professor

Department of Information Science and Engineering
Don Bosco Institute of Technology, Bengaluru,
India

Pin- 560074

Email- santhoshkumars.cs@gmail.com

Soumya L

Department of Information Science and Engineering
Don Bosco Institute of Technology, Bengaluru,
India

Pin- 560074

Email- soumyal2604@gmail.com

Shreya N Raj

Department of Information Science and Engineering
Don Bosco Institute of Technology, Bengaluru,
India

Pin- 560074

Email- shreya.nag452@gmail.com

Spandana N

Department of Information Science and Engineering
Don Bosco Institute of Technology, Bengaluru,
India

Pin- 560074

Email- spandanan876@gmail.com

Shushma S

Department of Information Science and Engineering
Don Bosco Institute of Technology, Bengaluru,
India

Pin- 560074

Email- shushmas165@gmail.com

Abstract: In response to the urgent need for swift and accurate diagnosis of COVID-19 during the global pandemic, there has been a growing interest in leveraging advanced technology like deep learning for detection purposes. This project introduces a novel approach termed COVID19-ResCapsNet, which integrates deep neural networks with X-ray imaging data to predict the likelihood of COVID-19 onset in patients. The methodology comprises two key steps. Initially, features are extracted using an enhanced Residual feature extraction network, aimed at capturing crucial information from the X-ray images. Subsequently, multiple Capsule Networks are employed to discern between COVID-19 and non-COVID-19 cases. This hybrid model is assessed using two separate datasets of chest X-ray images: Dataset-1 containing 50 images and Dataset-2 containing 20 images. Remarkably, the proposed method achieves high classification accuracy rates of 0.9988 on Dataset-1 and 0.9933 on Dataset-2 for binary classification tasks. To validate its efficacy, the performance of the COVID19-ResCapsNet model is compared against various state-of-the-art pre-trained classification models. Additionally, the study investigates the impact of two crucial hyper parameters: optimizer selection and batch size. The findings underscore the effectiveness of the proposed COVID-19 detection model, suggesting its potential as a complementary tool in clinical settings for expedited and accurate diagnosis.

Keywords: Deep learning, Capsule network, Residual network, COVID-19 detection.

1. Introduction

COVID-19, classified as a respiratory syndrome, spreads rapidly among humans through direct or indirect contact. It is characterized by a lengthy incubation period and can lead to various illnesses, as documented by multiple sources [1],[2]. According to the World Health Organization (WHO), common symptoms include cold, dry cough, and fever [3],[4]. Notably, a significant proportion of infected individuals, ranging from 40% to 50%, remain asymptomatic yet contagious [5],[6]. Transmission primarily occurs through respiratory droplets expelled during coughing or sneezing [7]. Given the absence of available drugs for prevention or treatment, early detection of infected individuals, followed by prompt quarantine and isolation measures, is essential for mitigating community transmission of COVID-19. Presently, the predominant diagnostic approach for COVID-19 involves real-time reverse transcriptase polymerase chain reaction (RT-PCR) [8]. This method typically employs nasopharyngeal swabs, oropharyngeal swabs, bronchoalveolar lavage fluid (BALF), and tracheal aspirates to isolate viral ribonucleic acid (RNA) from samples [9]. Despite its widespread use, RT-PCR testing is hampered by its time-consuming nature and high cost [10]. Moreover, it exhibits a lower detection rate and often necessitates stringent laboratory conditions, leading to delays in accurately diagnosing suspected cases [11].



Figure 1: Corona Virus

In contrast to RT-PCR, chest computed tomography (CT) scans and chest X-rays (CXRs) offer quicker and simpler alternatives for diagnosing COVID-19. They boast superior sensitivity in detecting the virus and are readily

available for widespread screening of suspected patients. In this study, CXRs are preferred over CT scans due to their widespread availability and lower cost in healthcare facilities. Additionally, CXRs expose patients to lower levels of ionizing radiation compared to CT scans. Therefore, we focus on analyzing chest X-ray images of COVID-19 as they provide a feasible imaging modality. Leveraging deep learning-based computer-aided diagnostic (CAD) techniques can expedite the analysis process and enhance the accuracy of COVID-19 detection. Thus, our objective is to develop an automated deep learning-based diagnostic method using chest X-ray images. The project introduces a novel network architecture, termed COVID19-ResCapsNet, integrating residual and capsule modules to achieve this goal.

CORONAVIRUS disease 2019 has been declared as a pandemic by the World Health Organization (WHO) a few months after its first appearance. It has infected more than 70 million people, caused a few million casualties, and has so far paralyzed mobility all around the world. The spreading rate of COVID-19 is so high that the number of cases is expected to be doubled every three days if the social distancing is not strictly observed to slow this accretion. Roughly around half of the COVID-19 positive patients also exhibit a comorbidity, making it difficult to differentiate COVID-19 from other lung disease. Automated and accurate COVID-19 diagnosis is critical for both saving [lives](#) and preventing its rapid spread in the community. Currently, reverse transcription-polymerase chain reaction (RT-PCR) and computed tomography (CT) are the common diagnostic techniques used today. RT-PCR results are ready at the earliest 24 h for critical cases and generally take several days to conclude a decision. CT may be an alternative at initial presentation; however, it is expensive and not easily accessible. The most common tool that medical experts use for both diagnostic and monitoring the course of the disease is X-ray imaging. Compared to RT-PCR or CT test, having an X-ray image is an extremely low cost and a fast process, usually taking only a few seconds. Recently, WHO reported that even RT-PCR may give false results in COVID-19 cases due to several reasons such as poor-quality specimen from the patient, inappropriate processing of the

specimen, taking the specimen at an early or late stage of the disease. For this reason, X-ray imaging has a great potential to be an alternative technological tool to be used along with the other tests for an accurate diagnosis. A real-time reverse transcriptase-polymerase chain reaction (RT-PCR) test is currently employed to detect COVID-19 cases. However, the test faces a critical problem of detecting false negatives and false positives, achieving sensitivity as low as nearly 60-70%. Moreover, the test process is labor-intensive and time-consuming and takes a long time to produce reports. Therefore, it generates a need for using other diagnostic approaches such as clinical investigation, computed tomography (CT), or x-ray imaging for detecting COVID-19 more quickly and effectively.

1.1 Problem statement

The problem at hand is the need for rapid and accurate detection of COVID-19 cases in the context of the ongoing pandemic. Current diagnostic methods are available, but the analysis of medical imaging, specifying chest X-ray scans, has shown promise in identifying potential COVID-19 cases. To improve this process, our research aims to develop COVID19-ResCapsNet, a novel deep learning architecture that combines the strengths of residual networks (ResNets) and capsule networks (CapsNets) to enhance the detection of COVID-19 from chest X-ray scans.

2. Literature Survey

The literature survey examines prior work in the field, focusing on addressing challenges inherent in the current system. It aims to equip users with a comprehensive understanding of these challenges and how to effectively address them. When contrasted with RT-PCR methods, both chest X-ray and CT scan images emerge as notably more effective and convenient. Furthermore, these images facilitate the diagnosis of the location and morphology of lung inflammation, making them indispensable tools in the detection of COVID-19. Numerous studies have demonstrated the accuracy and precision of diagnoses achieved through the analysis of these medical images. Recent advancements in CAD

techniques, particularly those based on deep learning, have demonstrated remarkable capabilities in identifying various disorders in chest radiographs, rivaling the accuracy of expert radiologists. These techniques, notably those employing convolutional neural networks (CNNs) [12], leverage unstructured data as input and aim to extract more meaningful features, thereby producing more precise results compared to traditional diagnostic methods.

Presently, CNN-based methods are extensively used to classify and evaluate chest X-ray (CXR) images or chest CT scans for COVID-19 detection, recognized as one of the most effective approaches [13]. These methods typically fall into two categories: utilizing medical imaging technologies like CT scans and CXRs, or employing RT-PCR technology for COVID-19 detection. Compared to RT-PCR methods, CXR and CT scan images offer greater efficiency and convenience, besides enabling the diagnosis of lung inflammation location and shape. Consequently, chest X-ray images and CT scans are predominantly employed in COVID-19 disease detection, with numerous studies reporting precise results using these medical images.

For instance, Wang et al. [14] proposed an Inception model, a deep convolutional-based neural network, which utilized patients' chest CT scan images for rapid COVID-19 detection, achieving 85% accuracy. Song et al. [15] introduced DRE-Net, a deep learning-based diagnosis network, achieving 86% sensitivity and 94% specificity on CT scan samples. Transfer learning on pre-trained CNNs was employed by Wang et al. [16] to categorize CXRs, achieving 93.3% accuracy. Nigam et al. [17] designed a COVID-19 diagnostic system using deep learning frameworks, achieving 93.48% accuracy in classifying COVID-19 positive, pneumonia, and normal cases. Afshar et al. [18] proposed COVID-CAPS network for COVID-19 detection with CXR images, achieving 95.7% accuracy in classification tasks. Furthermore, Apostolopoulos et al. [19] J. Lujan-Garcia et al. [20] and others have also reported significant accuracies ranging from 84% to 96.78% using CNN-based methods on CXR image datasets.

Despite these achievements, challenges persist. Some models face difficulties in parameter optimization, while others suffer from low accuracy or lack pre-processing for medical image datasets. To address these challenges, researchers are exploring lightweight residual network models, considering the limitations of common CNNs and the benefits of Capsule Networks (CapsNets) in capturing spatial information and reducing model complexity. CapsNets have shown promise in medical image processing, particularly in pneumonia detection. For instance, the COVID-FACT model utilizes CapsNets for COVID-19 detection, incorporating dynamic routing to identify spatial relations. However, it relies on radiologists to detect anomalies, leading to lower accuracy and inconvenience in application. To overcome this, COVID-CAPS was proposed, achieving an accuracy of 98.3% by leveraging CapsNets advantages in reduced parameter count and faster labeling processes. Nonetheless, training CapsNets often requires large datasets with uniform image sizes, necessitating significant time and hardware resources for preprocessing.

In conclusion, our exploration into the realm of COVID-19 and its implications for respiratory health, particularly through the lens of RESCAPS-NET, sheds light on the pressing need for innovative approaches in disease detection and management. As we navigate the complexities of this global pandemic, the development of novel technologies like RESCAPS-NET offers promising avenues for enhancing diagnostic accuracy and ultimately improving patient outcomes. However, while strides have been made, there remains much to uncover and refine in our understanding of COVID-19's impact on the respiratory system. Moving forward, continued collaboration, rigorous research, and technological innovation will be essential in addressing the challenges posed by COVID-19 and safeguarding public health worldwide.

3. COVID19 OF RESIDUAL CAPSULE NETWORK

A. THE COVID19-ResCapsNet MODEL

The framework diagram of our proposed COVID-19 ResCapsNet, presented in Fig. 1, comprises two main components. The first component is the residual feature extraction model (RFEM), responsible for extracting in-depth feature information from chest X-ray images, including texture features. Utilizing the residual structure, RFEM maintains the original shortcut connection while employing small convolution operations and identity mapping techniques to extract spatial features at varying depths for fusion. The second component, the capsule model (CM), primarily focuses on classifying chest X-ray images and identifying COVID-19 infection. The CM utilizes the Primary Capsule to transform scalar neurons into vector neurons and selectively triggers the advanced capsules within the Primary and Digital Capsule layers. Consequently, the recognition results of the Digital Capsules layer are attained.

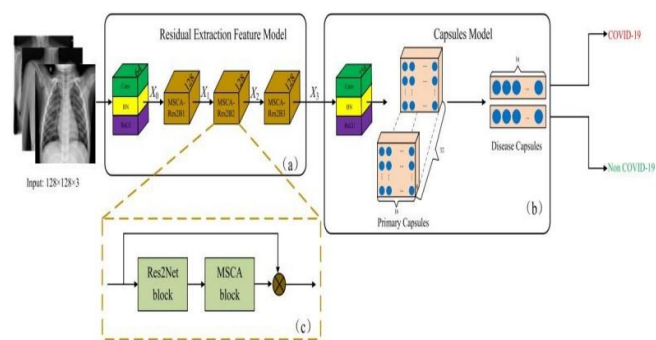


Figure 2: Structure of the proposed framework

This innovative framework efficiently and accurately identifies COVID19 cases and localizes infected areas within lung CT images. It also enhances the diagnostic precision, distinguishing COVID-19 and non-COVID-19 cases, ultimately facilitating timely and accurate disease identification.

B. RESIDUAL FEATURE EXTRACTION MODEL

1) Structure of RFEM

To enhance model performance while maintaining complexity, we employ residual learning to concatenate input and output. This approach allows for the preservation of more low-resolution features in the feature maps generated by higher layers, thus improving detection sensitivity. This study introduces the integration of the residual structure [25] into CapsNets [30], addressing issues such as loss of depth features or insufficient feature extraction.

The architecture of RFEM, depicted in Fig. 1(a), comprises three interconnected multi-scale channel attention Res2 blocks. Initially, the input image X undergoes processing with a 3×3 convolution ($\text{Conv}3 \times 3$) and zero-padding operation.

Subsequently, the results pass through the BN layer and activation layer using the ReLU function sequentially to obtain the shallow feature map X_0 , maintaining the same size as X . Finally, X_0 is input into three cascaded MSCA-Res2Bs to generate feature maps X_1 , X_2 , and X_3 , respectively. The mathematical expression for the shallow feature map X_0 is represented by the following equation:

$$X_0 = f \text{ReLU} (f \text{BN} (\text{Conv}3 \times 3 (X))) \quad (1)$$

Here, $\text{Conv}3 \times 3 (\cdot)$ denotes the 3×3 convolution operation, $f \text{BN} (\cdot)$ signifies batch normalization operation, and $f \text{ReLU} (\cdot)$ denotes the activation operation.

2) Structure of MSCA-Res2B

The REB block's structure, illustrated in Fig. 2(c) involves processing the shallow feature map X_0 through successive Res2Net and MSCA blocks. Subsequently, an 'Add' operation combines the output of the MSCA block with X_0 . In our Res2Net implementation, we utilize split and concatenation strategies to enhance the receptive field size of the output feature, enabling the

extraction of diverse global and local features at a fine-grained level across different scales. The MSCA block facilitates multi-channel attention fusion by altering the spatial set sizes.

To maintain model lightweightness and parameter reduction, this study incorporates local context information into the global context attention module. Additionally, PWConv serves as the local channel context information aggregator, leveraging spatial locations for point-by-point interaction.

3) Structure of Res2Net Block

In traditional convolutional feature transformation, the size of receptive fields is determined by the predefined convolution kernel size at each spatial position. This limitation hampers the network's ability to extract features effectively. To address this issue, we introduce the Res2Net block depicted in Fig. 2(a) to enlarge receptive fields and retain a broader range of features across various scales while minimizing parameter usage.

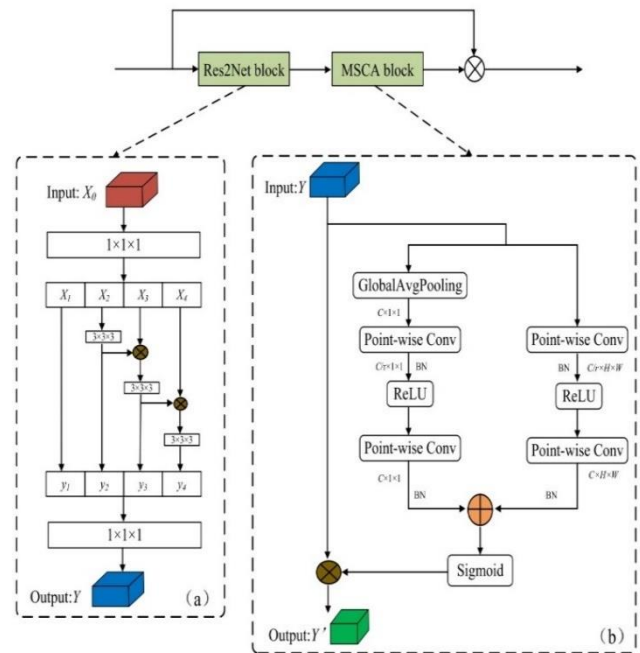


Figure 3. The architecture of the proposed Residual Extraction Blocks

Initially, the input feature map X_0 undergoes a 1×1 convolution layer instead of the original 3×3 convolution layer to capture both global and local contextual information from images. Subsequently, we evenly divide the resulting feature maps into m subsets, denoted as x_i (where $i = 1, 2, \dots, m$), each possessing the same size. For all subsets except the first (x_1), a corresponding 3×3 convolution operation, represented as f_i , is applied. The output of the convolution layer f_i is designated as y_i . We then combine each subset x_i with the output feature map of the preceding convolution layer, f_{i-1} , and feed the sum into f_i to obtain y_i . Consequently, y_i is computed as follows:

$$\begin{aligned} y_i &= \{x_i & \text{if } i = 1 \\ & f_i(x_i) & \text{if } i = 2 \\ & f_i(x_i + y_{i-1}) & \text{if } 2 < i \leq m \} \end{aligned} \quad (2)$$

Finally, for optimal fusion of information across different scales, all split subsets are concatenated and processed through a 1×1 convolution layer.

4) Structure of MSCA Block

The SENet module, as outlined in [36], focuses solely on extracting features of the same scale, relying on a consistent weight distribution. However, its reliance on global attention channels can lead to overlooking features of smaller targets. To address this limitation, this paper proposes a feature extraction method that considers two different scales. To maintain the lightweight nature of the MSCA block, we introduce PWConv as the local channel context information aggregator, which is integrated into the attention feature extractor. The structure of the MSCA block is depicted in Fig. 3(b), where two branches represent the global and local attention feature channels, respectively.

The extraction of local attention features can be expressed as follows:

$$L(Y) = \text{fBN}(\text{fPWConv2}(\text{fBN}(\text{fPWConv1}(Y)))) \quad (3)$$

Here, fPWConv denotes the 1×1 PWConv operation, which reduces the input feature's channel to $1/r$ of the original, with the resulting feature maintaining the original shape. r represents the scaling ratio. Other symbols correspond to Equ.1.

Additionally, our proposed method for extracting global attention features resembles SENet. However, to reduce computational costs, we substitute two original fully connected layers with PWConv. The global feature extraction process is represented as:

$$G(Y) = \text{fBN}(\text{fPWConv2}(\text{fReLU}(\text{fBN}(\text{fPWConv1}(\text{fGAP}(Y))))) \quad (4)$$

Here, GAP refers to global average pooling. Consequently, given the global attention feature $G(Y)$ and local attention feature $L(Y)$, the resulting feature Y' can be obtained through the MSCA block:

$$Y' = Y \otimes \text{MSCA}(Y) = Y \otimes \text{f sigmoid}(L(Y) \oplus G(Y)) \quad (5)$$

Here, $\text{MSCA}(Y)$ represents the attention weights, \oplus denotes broadcasting addition, and \otimes signifies element-wise multiplication.

C. CAPSULE NETWORKS

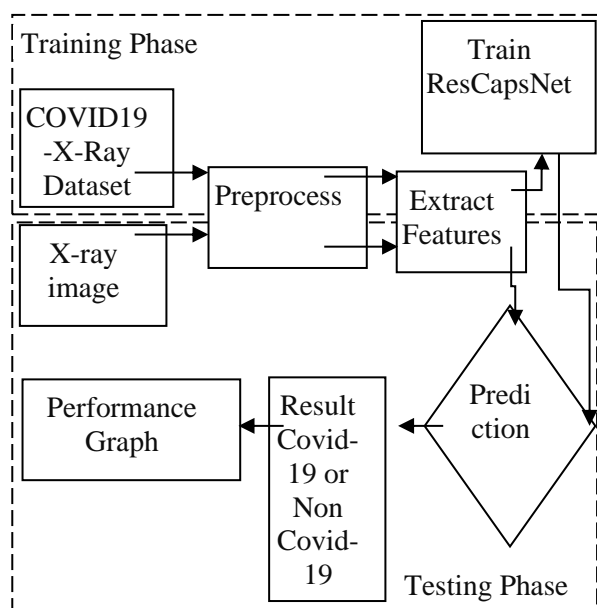
The Capsule Network approach replaces conventional neurons in CNNs with capsules, each representing a distinct image instance at a specific location. Capsules offer advantages over CNNs by encoding not only the probability of existence but also various characteristics like hue, texture, position, size, and direction, thereby enhancing classification and diagnosis performance.

Capsule Networks employ the "Protocol Routing Mechanism" to capture spatial information dynamically, determining the actual output of each capsule. Similar to conventional CNN modules, each capsule, equipped with corresponding instantiation parameters, predicts the output of the subsequent capsule layer.

Our proposed COVID19-ResCapsNet incorporates the Capsule part, as depicted in Fig. 2(b), within its architecture. This Capsule section comprises one convolutional layer, one batch-normalized layer, and three Capsule layers. The input to our COVID-Capsule Networks consists of X-ray images processed by our residual feature extraction model. The initial layer involves a convolutional operation followed by batch normalization and ReLU activation. Subsequently, three Capsule layers facilitate the routing by agreement process. The final Capsule layer contains instantiation parameters for two classes: positive and negative, indicating COVID-19 diagnosis. The lengths of these two Capsules signify the probability of each class's presence.

This paper introduces a novel network model based on the Capsule-Net framework tailored to handle small datasets effectively.

4. PROPOSED METHODOLOGY



We are implementing this project using following modules

List of modules:

1. Data Collection
2. Data preprocessing

3. Building and training RESNET-50, models
4. Prediction of COVID
5. Detection of Infected Area

Module Description:

1. Data Collection:

We are collecting the COVID chest X-ray image dataset from kaggle.com. Our dataset Contains two types of classes COVID sever or COVID non-sever. Each class contains 1100 images.

2. Data Preprocessing:

The collected dataset images will be in different size so we need to change into the fixed size to given the input to the training model so we are using the open cv resize function to change into fixed size of 224x244.

Preprocessing of the Chest X-Ray Scan images:

Image Resizing and Rescaling: Resizing and rescaling images can be a helpful preprocessing step in various applications, including those related to COVID-19 research or any other image-based analysis. The techniques employed are:

1. Load Images: Import libraries like OpenCV or PIL to load the images into your Python environment.
2. Resize Images: Use the resize function from the chosen library to resize the images to a standard size. Specify the desired dimensions for resizing.
3. Rescale Pixel Values: Determine the range to which you want to rescale the pixel values. This could be 0 to 1 or -1 to 1, depending on your preference and the requirements of your model.
4. Normalize Pixel Values: Calculate the mean and standard deviation of the pixel values across all images. Then, subtract the mean from each pixel value and divide by the standard deviation. This step helps in standardizing the pixel values and improving convergence during training.

Pseudocode for Image Resizing and Rescaling

```
Function_resize_and_rescale_image(image,  
new_size):
```

```
import image_processing_library as img_lib
```

```
resized_image=          img_lib.resize(image,  
new_size)
```

```
rescaled_image=img_lib.rescale(resized_imag  
e)
```

```
return rescaled_image
```

3. Building And Training of RESNET50 :

Resnet Architecture: The proposed deep RESNET-50 network will be trained on the processed dataset. RESNET-50 is used especially in multiclass classification. It is a special kind of Recurrent Neural Networks (RNN) that could learn long-term dependencies.

Import pretrained ResNet model specifying desired variant (e.g., ResNet50) using TensorFlow or PyTorch. Access last convolutional layer and remove fully connected layers to exclude original classifier. Define new layers for COVID-19 detection, typically involving fully connected layers followed by sigmoid output. Train model using preprocessed images and corresponding labels (0 for COVID positive, 1 for non-COVID) with specified epochs and batch size. Evaluate model performance on separate validation set, monitoring metrics like accuracy, precision.

Pseudocode for a ResNet architecture

- Procedure Building and Training()
- Input: Image features
- Output: Pre-trained model
- Begin:

- Step1: Read features.
- Step2: Build the RESNET-50 model
- Step3: Split data into train and test
- Step4: Train the data
- Return pre-trained model
- End

4. Prediction of COVID severity:

To classify COVID-19 and Non COVID-19 patients:

COVID-19 Classification with CNN:

To distinguish between COVID-19 positive and non-COVID-19 cases, employ a ResNet 50 architecture coupled with a Convolutional Neural Network (CNN). Evaluate the model's efficacy by assessing its performance on a separate test dataset. Metrics like accuracy and precision be utilized for this evaluation, providing insights into the model's ability to correctly classify images.

This project proposed a deep RESNET-50 technique to detect the COVID-19 severity from the input chest x-ray images using resnet. Performance results prove that the proposed scheme yielded the highest accuracy, over more than 98%, compared to the others in which the RESNET-50 is used as a single model without any combination.

Pseudocode for COVID-19 Classification with RESNET-50 coupled with CNN:

- Procedure Prediction()
- Input: image
- Output: COVID severity
- Begin:

- Step1: Read frame.
- Step2: Load RESNET-50 model
- Step3: Preprocess the input frame
- Step4: Predict the COVID-19 is there or not
- Step5: Detect the infected region and predict the level of COVID-19 level and recommend the treatment.
- End

5. Detection of Infected Area:

Gaussian Blurring, Watershed Algorithm, Morphological Functions

1. Gaussian Blurring: Gaussian blurring is a technique used to reduce noise and detail in an image by applying a Gaussian filter. The filter convolves the image with a Gaussian kernel, which assigns weights to neighboring pixels based on their distance from the center.

Pseudocode for Gaussian Blurring

```
function gaussian_blur(image, kernel_size, sigma):
```

```
    blurred_image = apply_gaussian_filter(image, kernel_size, sigma)
```

```
    return blurred_image
```

2. Watershed Algorithm:

The watershed algorithm is a segmentation technique used to identify and separate objects or regions in an image. It treats the pixel intensity values as topographic features and simulates a flooding process from local minima.

Pseudocode for Watershed Algorithm

```
function apply_markers(image):
```

```
    markers = detect_markers(image)
```

```
    return markers
```

```
function watershed_algorithm(image, markers):
```

```
    segmented_image = apply_watershed(image, markers)
```

```
    return segmented_image
```

3. Morphological Functions:

Morphological functions are mathematical operations used for analyzing and processing geometric structures in images. Common morphological operations include dilation, erosion, opening, and closing.

Pseudocode for Morphological Functions

```
function dilation(image, kernel):
```

```
    dilated_image = apply_dilation(image, kernel)
```

```
    return dilated_image
```

```
function erosion(image, kernel):
```

```
    eroded_image = apply_erosion(image, kernel)
```

```
    return eroded_image
```

```
function opening(image, kernel):
```

```
    opened_image = erosion(image, kernel)
```

```
    opened_image = dilation(opened_image, kernel)
```

```
    return opened_image
```

```
function closing(image, kernel):
```

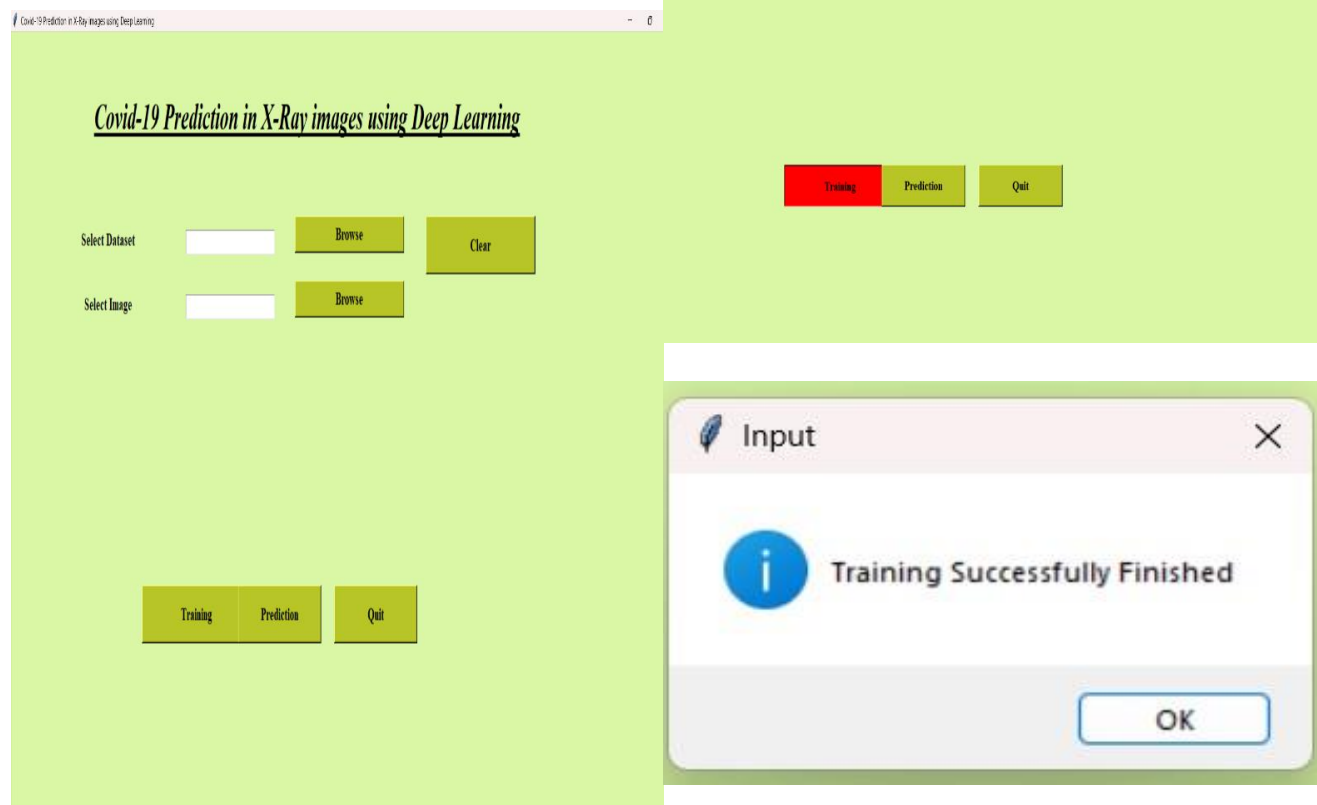
```
    closed_image = dilation(image, kernel)
```

```
    closed_image = erosion(closed_image, kernel)
```

return closed_image

5. Results and discussion

GUI for Covid-19 Training and Prediction By using X-Ray images as Dataset

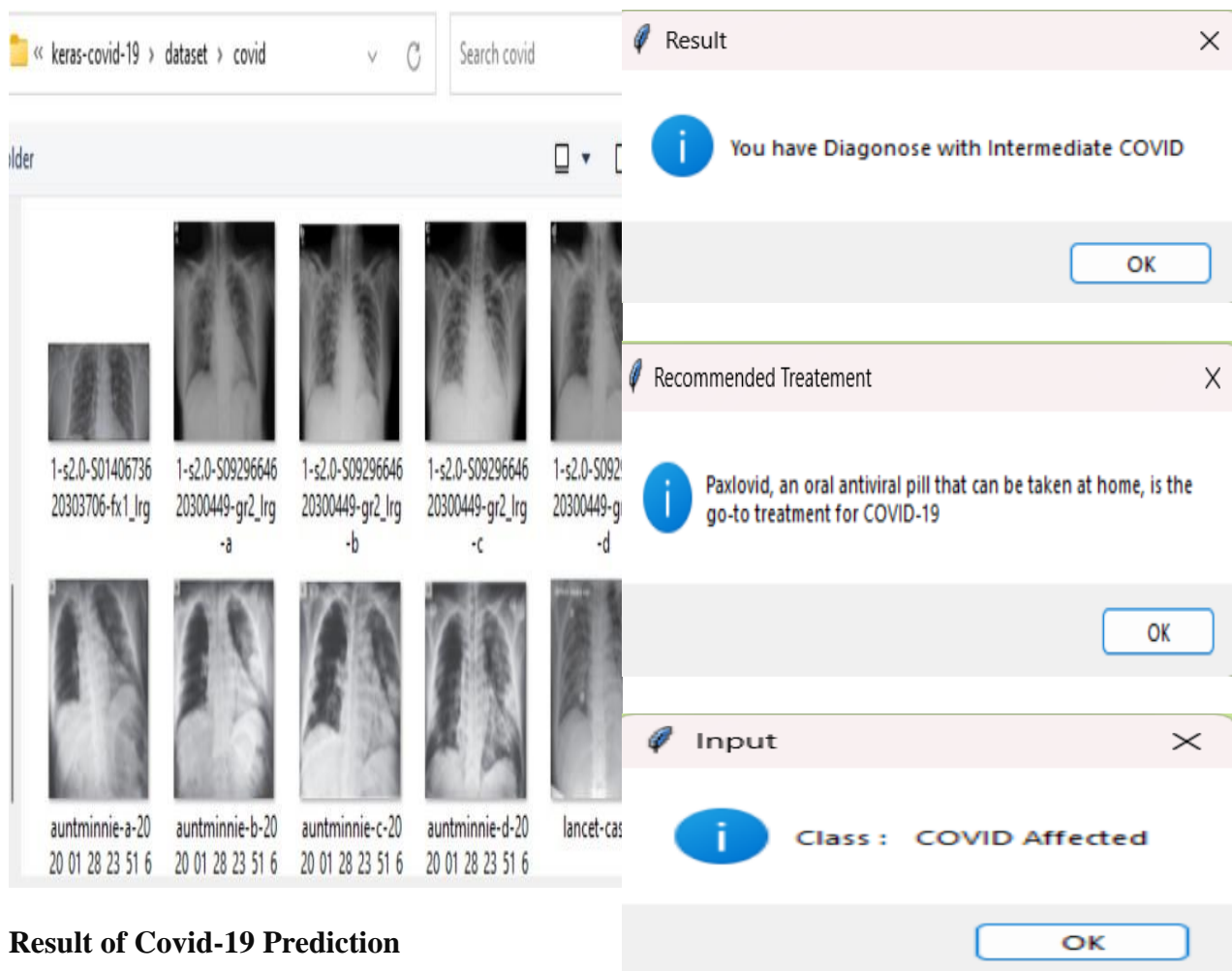


A GUI for COVID-19 training and prediction utilizing X-ray images as a dataset offers an intuitive interface for users to train and predict COVID-19 cases based on X-ray images. Users can upload X-ray datasets, select training parameters, and visualize training progress. After training, the GUI allows for real-time prediction of new X-ray images, providing rapid and accessible assistance in diagnosing COVID-19 cases.

Selecting Dataset for Covid-19 Prediction

Projectcode > keras-covid-19 > dataset			
Search dataset			
Name	Date modified	Type	Size
covid	22-04-2024 13:44	File folder	
normal	22-04-2024 13:44	File folder	

Process of Training the Dataset of Covid-19

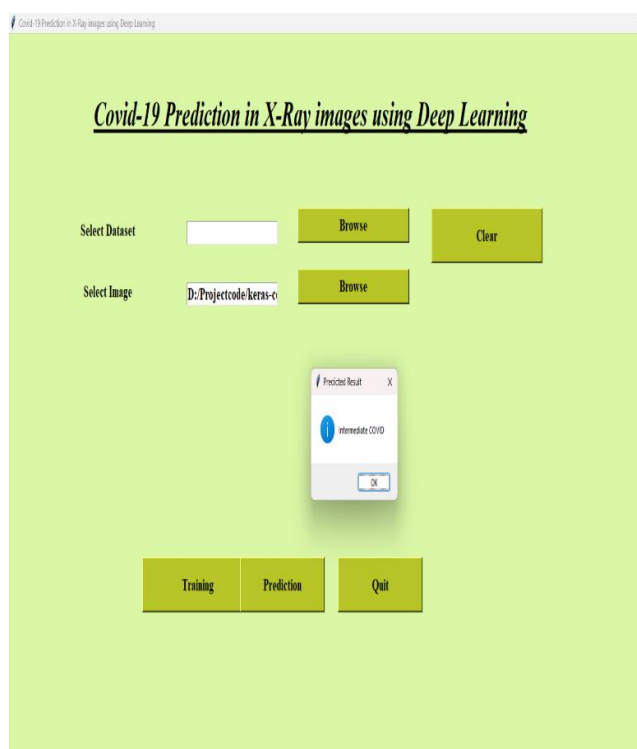


The screenshot displays a software interface for COVID-19 prediction. On the left, a file explorer shows a directory structure: « keras-covid-19 » dataset » covid. Below this, a grid of X-ray images is shown, each with a label and a date. The labels include '1-s2.0-S01406736 20303706-fx1_lrg', '1-s2.0-S09296646 20300449-gr2_lrg', '1-s2.0-S09296646 20300449-gr2_lrg', '1-s2.0-S09296646 20300449-gr2_lrg', '1-s2.0-S09296646 20300449-gr2_lrg', 'auntminnie-a-20 20 01 28 23 51 6', 'auntminnie-b-20 20 01 28 23 51 6', 'auntminnie-c-20 20 01 28 23 51 6', 'auntminnie-d-20 20 01 28 23 51 6', and 'lancet-cas'. On the right, there are three panels. The top panel, titled 'Result', shows a message: 'You have Diagnose with Intermediate COVID' with an 'OK' button. The middle panel, titled 'Recommended Treatment', shows a message: 'Paxlovid, an oral antiviral pill that can be taken at home, is the go-to treatment for COVID-19' with an 'OK' button. The bottom panel, titled 'Input', shows a message: 'Class : COVID Affected' with an 'OK' button.

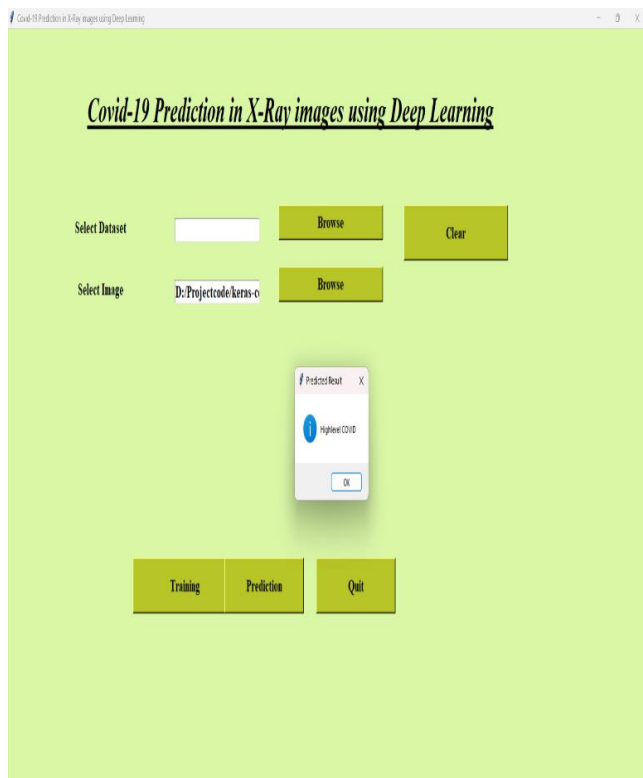
Result of Covid-19 Prediction

For Intermediate Level COVID-19

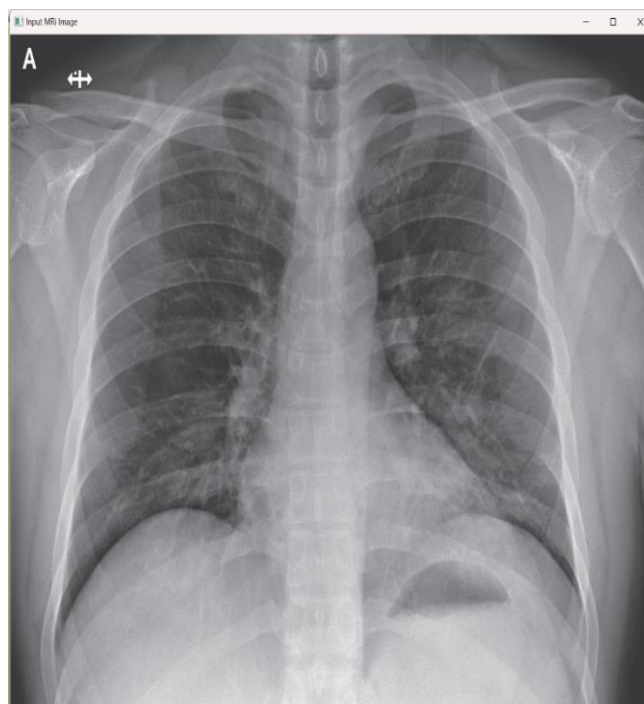
For High Level COVID-19



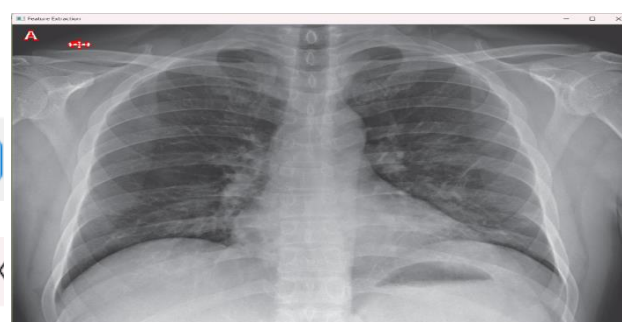
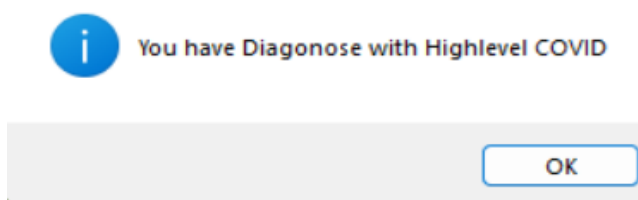
The screenshot displays a software interface for COVID-19 prediction. The title is 'Covid-19 Prediction in X-Ray images using Deep Learning'. Below the title, there are two sections for file selection. The first section, 'Select Dataset', has a text box and a 'Browse' button. The second section, 'Select Image', has a text box containing 'D:\Projectcode\keras-o' and a 'Browse' button. At the bottom, there are three buttons: 'Training', 'Prediction', and 'Quit'. A small window titled 'Predicted Result' is open, showing a message: 'Intermediate COVID' with an 'OK' button.



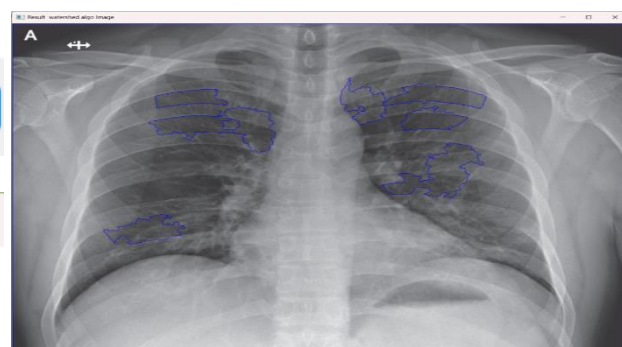
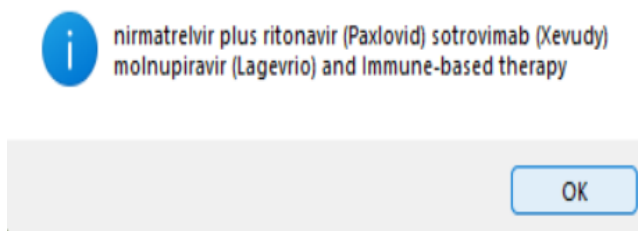
Input MRI image



Feature Extraction



Result of watershed algorithm

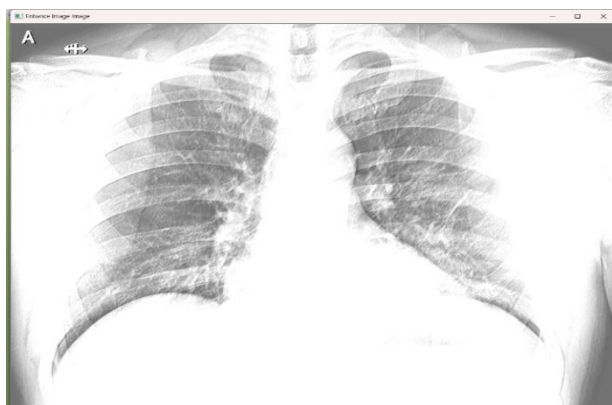


Gray Image

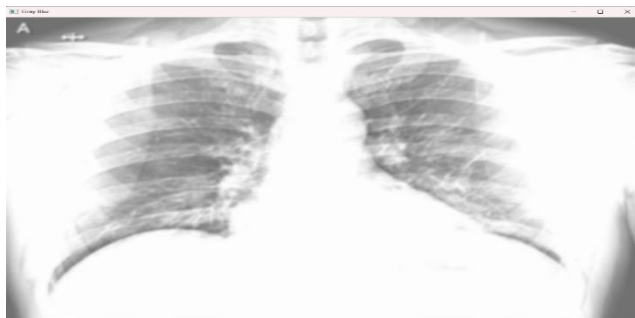
Levels of identifying the infected area



Enhance Image



Gray Blur Image



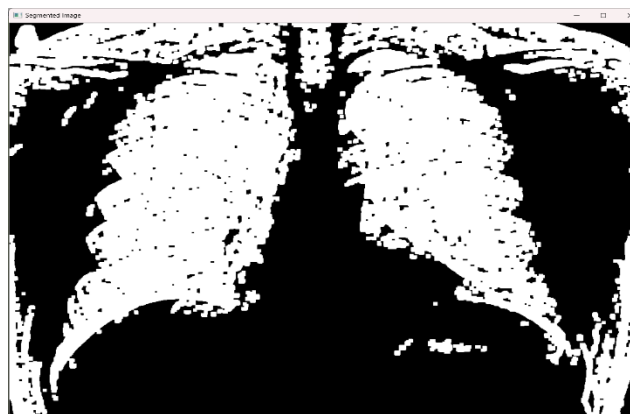
Threshold Image



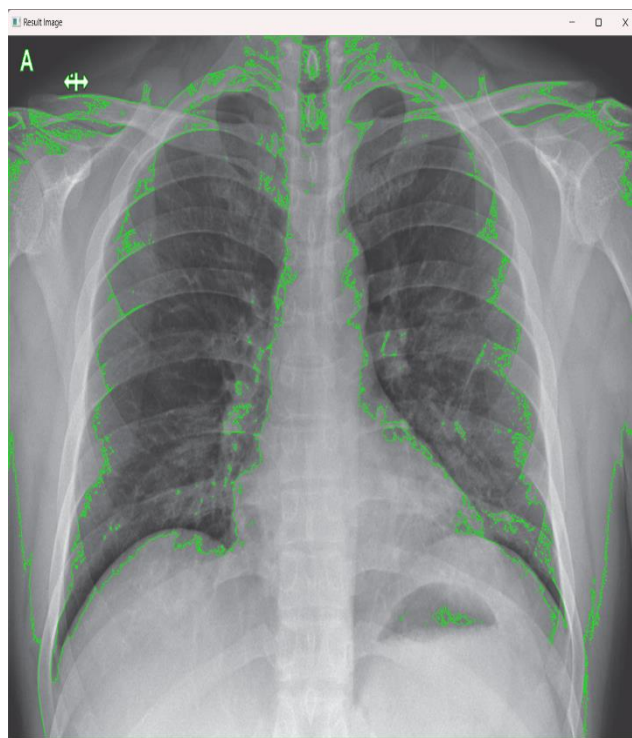
Kernal Image



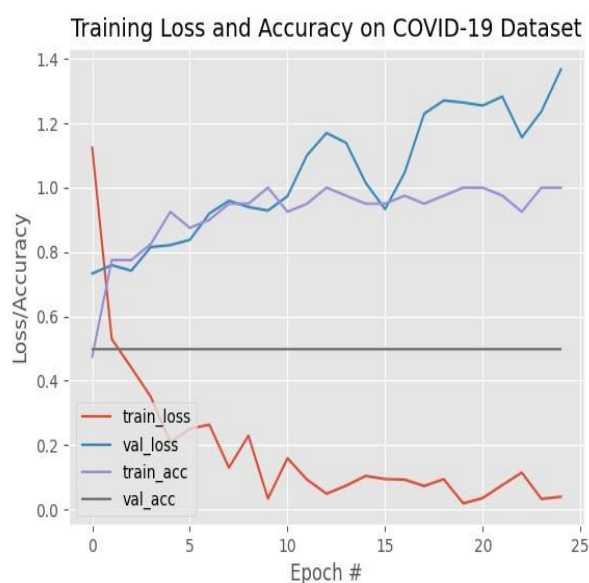
Segmented Image



Result Image



An effective and efficient COVID-19 detection system has been implemented, accurately identifying COVID-19 cases and localizing infected areas within lung CT images. COVID-19 ResCapsNet system yields positive detection results for COVID-19 cases and negative detection results for non-COVID-19 cases, enhancing the precision and timeliness of diagnostics. It also provides the level of risk and recommends the medication to the Covid-19 patients.



In the COVID-19 dataset, training loss and accuracy show a dynamic relationship. Initially, loss decreases as accuracy improves steadily, reflecting model learning. However, fluctuations may occur due to dataset variability or model complexity. Eventually, both metrics stabilize, indicating optimal model performance, crucial for reliable predictions in public health responses.

6. Conclusion and future scope

This paper would summarize the findings and effectiveness of the ResCapsNet model in detecting COVID-19. It would likely discuss the accuracy, sensitivity, limitations, potential future improvements, the significance of the finding for combating the pandemic and specificity of the model compared to existing methods.

As for future scope, it could include further

refining the model with more data for enhanced accuracy, exploring its potential for real-time detection in healthcare settings, adapting it to detect new variants of the virus, and potentially integrating it into diagnostic tools or applications for wide spread use in communities.

Conflicts of interest

There are no conflicts of interest declared by any of the authors.

Acknowledgment

We acknowledge everyone for supporting me for doing research.

Author contributions

Authors proposed a task like conceptualizing the ResCapsNet model, designing the architecture, implementing the algorithm, collecting and preprocessing data, conducting experiments, analyzing results, and writing the paper.

Each author might have contributed differently, but collectively they would have contributed to various aspects of the project, including its development and dissemination.

References

- [1] C.Wu, "Risk factors associated with acute respiratory distress syndrome and death in patients with coronavirus disease 2019 pneumonia in Wuhan, China," *Jama Internal Med.*, vol. 180, no. 7, pp. 934–943, Apr. 2020.
- [2] N. M. da Costa et al., "Dashboard COMPRIME_COMPRI_MOv: Multiscale spatio-temporal monitoring of the COVID-19 pandemic in Portugal," *Future Internet*, vol.13, no. 2, pp. 45, Feb. 2021.
- [3] N. Chen, M. Zhou et al., "Epidemiological and clinical characteristics of 99 cases of 2019 novel coronavirus pneumonia in Wuhan, China: A descriptive study," *Lancet*, vol. 395, no. 10223, pp. 507–513, Feb. 2020.
- [4] W.Zhang, "Imaging changes of severe COVID-19 pneumonia in advanced stage," *Intensive Care Med.*, vol. 46, no. 5, pp. 841–

- 843, May 2020.
- [5] M. Cevik, I. I. Bogoch et al., "Prevalence of asymptomatic SARS-CoV-2 infection," *Ann. Internal Med.*, vol. 174, no. 2, pp. 283–284, Feb. 2021.
 - [6] S. Ecks, "Multimorbidity, polyiatrogenesis, and COVID-19," *Med. Anthropology Quart.*, vol. 34, no. 4, pp. 488–503, Dec. 2020.
 - [7] S. K. Greene, S. F. McGough et al., "Nowcasting for real-time COVID-19 tracking in New York city: An evaluation using reportable disease data from early in the pandemic," *JMIR Public Health Surveill.*, vol. 7, no. 1, pp. 180–188, Jan. 2021.
 - [8] J. Wu, J. Liu et al., "Detection and analysis of nucleic acid in various biological samples of COVID-19 patients," *Travel Med. Infectious Disease*, vol. 37, no.2, pp.23, Sep. 2020.
 - [9] V. M. Corman et al., "Detection of 2019 novel coronavirus(2019-nCoV) by real-time RT-PCR," *Euro Surveill*, vol. 25, no. 3, pp. 23–30, Jan. 2020.
 - [10] C. P. West, V. M. Montori et al., "COVID-19 testing: The threat of false-negative results," *Mayo Clinic Proc.*, vol. 95, no. 6, pp. 1127–1129, Jun. 2020.
 - [11] E. Dong, H. Du et al., "An interactive web-based dashboard to track COVID-19 in real time," *Lancet Infectious Diseases*, vol. 20, no. 5, pp. 533–534, May 2020.
 - [12] P.H. Dinh, "A novel approach based on three-scale image decomposition and marine predators' algorithm for multi-modal medical image fusion," *Biomed. Signal Process. Control*, vol. 67, no.8, pp. 134, May 2021.
 - [13] H. Panwar, P. K. Gupta et al., "A deep learning and grad-CAM based color visualization approach for fast detection of COVID-19 cases using chest Xray and CT-scan images," *Chaos, Solitons Fractals*, vol. 140, no.11, pp.23, Nov. 2020.
 - [14] S. Wang, B. Kang et al., "A deep learning algorithm using CT images to screen for corona virus disease (COVID-19)," *Eur. Radiol.*, vol. 31, no. 8, pp. 6096–6104, Feb. 2021.
 - [15] Y. Song, S. Zheng et al., "Deep learning enables accurate diagnosis of novel coronavirus (COVID-19) with CT images," *IEEE/ACM Trans. Comput. Biol.Bioinf.*, vol. 18, no. 6, pp. 2775–2780, Nov. 2021.
 - [16] L.Wang,Z. Q.Lin, et al., "COVID-net: A tailored deep convolutional neural network design for detection of COVID-19 cases from chest X-ray images," *Sci. Rep.*, vol. 10, no. 1, Nov. 2020.
 - [17] B.Nigam,R.Jain, et al., "COVID-19: Automatic detection from X-ray images by utilizing deep learning methods," *Exp. Syst. Appl.*, vol. 176, Aug. 2021.
 - [18] P.Afshar et al., , "COVID-CAPS: A capsule network-based framework for identification of COVID-19 cases from X-ray images," *Pattern Recognit. Lett.*, vol. 138, pp. 638–643, Oct. 2020.
 - [19] I.D.Apostolopoulos s and T. A. Mpesiana, "Covid-19: Automatic detection from X-ray images utilizing transfer learning with convolutional neural networks," *Phys. Eng. Sci. Med.*, vol. 43, no. 2, pp. 635–640, Jun. 2020.
 - [20] J. Luján-García, C. Yáñez-Márquez et al., "A transfer learning method for pneumonia classification and visualization," *Appl. Sci.*, vol. 10, no. 8, p. 2908, Apr. 2020.
 - [21] M. Togaçar, B. Ergen, and Z. Cömert, "COVID-19 detection using deep learning models to exploit social mimic optimization and structured chest X-ray images using fuzzy color and stacking approaches," *Comput. Biol. Med.*, vol. 121, Jun. 2020.
 - [22] T. Ozturk, M. Talo, E. A. Yildirim et al., "Automated detection of COVID-19 cases using deep neural networks with X-ray images," *Comput. Biol. Med.*, vol. 121, Jun. 2020.
 - [23] S. Kumar, S. Mishra, and S. K. Singh, "Deep transfer learning-based COVID-19 prediction using chest X-rays," *J. Health Manage.*, vol. 23, no. 4, pp. 730–746, Dec. 2021.
 - [24] F. Wu, J. Yuan, Y. Li, J. Li, and M. Ye, "ASA-CoroNet: Adaptive selfattention network for COVID-19 automated diagnosis using chest Xray images," in *Proc. 1st Workshop Healthcare AI COVID-19 (ICML)*, Baltimore, MD, USA, 2020, pp. 11–20.
 - [25] K. He, X. Zhang, S. Ren, and J. Sun, "Deep residual learning for image recognition," in

- Proc. IEEE Conf. Comput. Vis. Pattern Recognit. (CVPR), Las Vegas, NV, USA, Jun. 2016, pp. 770–778.
- [26] L. Li, L. Qin, Z. Xu et al., “Artificial intelligence distinguishes COVID-19 from community acquired pneumonia on chest CT,” *Radiology*, vol. 296, no. 2, pp. E65–E72, Apr. 2020.
- [27] A. A. Ardakani, A. R. Kanafi et al., “Application of deep learning technique to manage COVID-19 in routine clinical practice using CT images: Results of 10 convolutional neural networks,” *Comput. Biol. Med.*, vol. 121, Jun. 2020.
- [28] M. Rahimzadeh and A. Attar, “A modified deep convolutional neural network for detecting COVID-19 and pneumonia from chest X-ray images based on the concatenation of xception and ResNet50 V2,” *Informat. Med. Unlocked*, vol. 19, 2020.
- [29] E. M. El-Kenawy, S. Mirjalili et al., “Advanced meta-heuristics, convolutional neural networks, and feature selectors for efficient COVID-19 X-ray chest image classification,” *IEEE Access*, vol. 9, pp. 36019–36037, 2021.
- [30] G. E. Hinton, S. Sbour, and N. Frosst, “Matrix capsules with EM routing,” in *Proc. Int. Conf. Learn. Represent. (ICLR)*, Vancouver, BC, Canada, 2018, pp. 1–15.
- [31] P. Afshar, K. N. Plataniotis, and A. Mohammadi, “BoostCaps: A boosted capsule network for brain tumor classification,” in *Proc. 42nd Annu. Int. Conf. IEEE Eng. Med. Biol. Soc. (EMBC)*, Montreal, BC, Canada, Jul. 2020, pp. 1075–1079.
- [32] P. Afshar, A. Mohammadi, and K. N. Plataniotis, “BayesCap: A Bayesian approach to brain tumor classification using capsule networks,” *IEEE Signal Process. Lett.*, vol. 27, pp. 2024–2028, 2020.
- [33] P. Afshar, A. Oikonomou, F. Naderkhani et al., “3D-MCN: A 3D multi-scale capsule network for lung nodule malignancy prediction,” *Sci. Rep.*, vol. 10, no. 1, p. 7948, May 2020.
- [34] S. Heidarian, P. Afshar et al., “COVID-FACT: A fully-automated capsule networkbased framework for identification of COVID-19 cases from chest CT scans,” *Frontiers Artif. Intell.*, vol. 4, May 2021.
- [35] S. Toraman, T. B. Alakus, and I. Turkoglu, “Convolutional capsnet: A novel artificial neural network approach to detect COVID-19 disease from X-ray images using capsule networks,” *Chaos, Solitons Fractals*, vol. 140, Nov. 2020.
- [36] J. Hu, L. Shen, S. Albanie, G. Sun, and E. Wu, “Squeeze-and-excitation networks,” *IEEE Trans. Pattern Anal. Mach. Intell.*, vol. 42, no. 8, pp. 2011–2023, Aug. 2020.
- [37] J. P. Cohen. Covid Chest X-Ray Dataset. Accessed: Mar. 10, 2023. [Online]. Available: <https://github.com/ieee8023/covid-chestxray-dataset>
- [38] D. S. Kermany, “Identifying medical diagnoses and treatable diseases by image-based deep learning,” *Cell*, vol. 172, no. 5, pp. 1122–1131, Feb. 2018.
- [39] A. Ashutosh, V. Ankur, S. Anshuman. COVID-19_XRay_Classifier Accessed: Mar. 10, 2023. [Online]. Available: https://github.com/AshuMaths1729/COVID-19_XRay_C-classifier
- [40] Z. Lin, Z. He, S. Xie et al., “AANet: Adaptive attention network for COVID-19 detection from chest X-ray images,” *IEEE Trans. Neural Netw. Learn. Syst.*, vol. 32, no. 11, pp. 4781–4792, Nov. 2021.
- [41] M. Roberts, D. Driggs et al., “Common pitfalls and recommendations for using machine learning to detect and prognosticate for COVID19 using chest radiographs and CT scans,” *Nature Mach. Intell.*, vol. 33, pp. 199–217, Mar. 2021.
- [42] M. Umer, I. Ashraf et al., “COVINet: A convolutional neural network approach for predicting COVID-19 from chest X-ray images,” *J. Ambient Intell. Humanized Comput.*, vol. 13, no. 1, pp. 535–547, Jan. 2021.
- [43] K. H. Shibly, S. K. Dey et al., “COVID faster R-CNN: A novel framework to diagnose novel coronavirus disease (COVID-19) in X-ray images,” *Informat. Med. Unlocked*, vol. 20, 2020.
- [44] H. Nasiri and S. Hasani, “Automated detection of COVID-19 cases from chest X-ray

- images using deep neural network and XGBoost,” *Radiography*, vol. 28, no. 3, pp. 732–738, Aug. 2022.
- [45] Y. E. Almalki, A. Qayyum et al., “A novel method for COVID19 diagnosis using artificial intelligence in chest X-ray images,” *Healthcare*, vol. 9, no. 5, p. 522, Apr. 2021.
- [46] N. Ullah, J. A. Khan, S. Almakdi et al., “A novel CovidDetNet deep learning model for effective COVID-19 infection detection using chest radiograph images,” *Appl. Sci.*, vol. 12, no. 12, p. 6269, Jun. 2022.
- [47] S. Kumar, V. Mansotra et al., “LiteCovidNet: A lightweight deep neural network model for detection of COVID-19 using X-ray images,” *Int. J. Imag. Syst. Technol.*, vol. 32, no. 5, pp. 1464–1480, Sep. 2022.
- [48] N. Narayan Das, N. Kumar et al., “Automated deep transfer learning-based approach for detection of COVID-19 infection in chest X-rays,” *IRBM*, vol. 43, no. 2, pp. 114–119, Apr. 2022.
- [49] A. Mustapha, L. Mohamed, and K. Ali, “An overview of gradient descent algorithm optimization in machine learning: Application in the ophthalmology field,” in *Proc. Int. Conf. Smart Appl. Data Analysis (SADASC)*, Marrakesh, MA, USA, 2020, pp. 25–26.
- [50] J. Duchi, E. Hazan, and Y. Singer, “Adaptive subgradient methods for online learning and stochastic optimization,” *J. Mach. Learn. Res.*, vol. 12, pp. 2121–2159, Feb. 2011.
- [51] I. Sutskever, J. Martens et al., “On the importance of initialization and momentum in deep learning,” in *Proc. 30th Int. Conf. Int. Conf. Mach. Learn.*, Atlanta, GA, USA, 2013, pp. 1139–1147.
- [52] M.-H. Guo, M.-M. Cheng et al., “Attention mechanisms in computer vision: A survey,” *Comput. Vis. Media*, vol. 8, pp. 331–368, Mar. 2022.
- [53] G. Huang, Z. Liu, L. Van Der Maaten, and K. Q. Weinberger, “Densely connected convolutional networks,” in *Proc. IEEE Conf. Comput. Vis. Pattern Recognit. (CVPR)*, Hawaii, HI, USA, Jul. 2017, pp. 2261–2269.
- [54] F. Chollet, “Xception: Deep learning with depthwise separable convolutions,” in *Proc. IEEE Conf. Comput. Vis. Pattern Recognit. (CVPR)*, Hawaii, HI, USA, Jul. 2017, pp. 1800–1807.
- [55] J. van der Laak, G. Litjens, and F. Ciompi, “Deep learning in histopathology: The path to the clinic,” *Nature Med.*, vol. 27, no. 5, pp. 775–784, May 2021.
- [56] K. He, X. Zhang, S. Ren, and J. Sun, “Deep residual learning for image recognition,” in *Proc. IEEE Conf. Comput. Vis. Pattern Recognit. (CVPR)*, Las Vegas, NV, USA, Jun. 2016, pp. 770–778.
- [57] A. Krizhevsky, I. Sutskever, and G. E. Hinton, “ImageNet classification with deep convolutional neural networks,” *Commun. ACM*, vol. 60, no. 6, pp. 84–90, May 2017.
- [58] Y. Wu, S. Gao, J. Mei, J. Xu, D. Fan, R. Zhang, and M. Cheng, “JCS: An explainable COVID-19 diagnosis system by joint classification and segmentation,” *IEEE Trans. Image Process.*, vol. 30, pp. 3113–3126, Feb. 2021.